analytical chemistry

Article

Cite This: Anal. Chem. XXXX, XXX, XXX−XXX

pubs.acs.org/ac

# Detection of Extended-Spectrum β-Lactamase-Producing *Escherichia coli* Using Infrared Microscopy and Machine-Learning Algorithms

Uraib Sharaha,[†] Eladio Rodriguez-Diaz,[‡] Orli Sagi,[§] Klaris Riesenberg,[∥] Itshak Lapidot,[⊥] Yoram Segal,[#] Irving J. Bigio,[▲,‡,▽] Mahmoud Huleihel,*[,▲,†] and Ahmad Salman*[,▲,¶]

[†]Department of Microbiology, Immunology and Genetics and [#]Department of Communication Systems Engineering, Ben-Gurion University of the Negev, Beer-Sheva 84105, Israel

[‡]Department of Biomedical Engineering and [▽]Department of Electrical & Computer Engineering, Boston University, Boston, Massachusetts 02215, United States

[§]Director of Microbiology Laboratory, Soroka University Medical Center, Beer-Sheva 84105, Israel

[∥]Soroka University Medical Center, Beer-Sheva 84105, Israel

[⊥]Department of Electrical and Electronics Engineering, ACLP-Afeka Center for Language Processing, Afeka Tel-Aviv Academic College of Engineering, Tel-Aviv 69107, Israel

[¶]Department of Physics, SCE - Shamoon College of Engineering, Beer-Sheva 84100, Israel

Supporting Information

**ABSTRACT:** The spread of multidrug resistant bacteria has become a global concern. One of the most important and emergent classes of multidrug-resistant bacteria is extended-spectrum β-lactamase-producing bacteria (ESBL-positive = ESBL$^+$). Due to widespread and continuous evolution of ESBL-producing bacteria, they become increasingly resistant to many of the commonly used antibiotics, leading to an increase in the mortality associated with resulting infections. Timely detection of ESBL-producing bacteria and rapid determination of their susceptibility to appropriate antibiotics can reduce the spread of these bacteria and the consequent complications. Routine methods used for the detection of ESBL-producing bacteria are time-consuming, requiring at least 48 h to obtain results. In this study, we evaluated the potential of infrared spectroscopic microscopy, combined with multivariate analysis for rapid detection of ESBL-producing *Escherichia coli* (*E. coli*) isolated from urinary-tract infection (UTI) samples. Our measurements were conducted on 837 samples of uropathogenic *E. coli* (UPEC), including 268 ESBL$^+$ and 569 ESBL-negative (ESBL$^-$) samples. All samples were obtained from bacterial colonies after 24 h culture (first culture) from midstream patients' urine. Our results revealed that it is possible to detect ESBL-producing bacteria, with a 97% success rate, 99% sensitivity, and 94% specificity for the tested samples, in a time span of few minutes following the first culture.

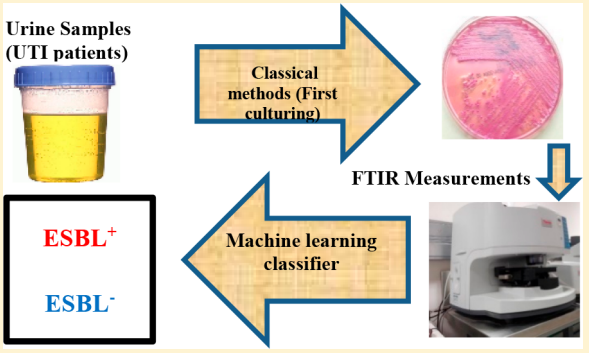




β-Lactams are the most widely used class of antibiotics, including penicillins, cephalosporins, carbapenems, monobactams, and cephamycins.[1] These antibiotics are characterized by having a β-lactam ring, which effects the bactericidal activity by ligating to penicillin-binding proteins and inhibiting the synthesis of the bacterial peptidoglycan cell wall.

ESBL is one group of β-lactamase enzymes that are produced by a variety of Gram-negative bacteria, leading to inactivation of β-lactam antibiotics by hydrolysis.[2] Since the first report of ESBL$^+$ organisms in the 1980s, these organisms have received increasing attention because bacteria with ESBL are resistant to more than 40 antibiotics.[2]

Moreover, with the lack of new antibiotics, the spread of ESBL-producing bacteria becomes a growing problem,[3−6] leading to an increase in the mortality rate associated with ESBL-producing bacterial infections.[7] Even though the major ESBL-producing organisms isolated worldwide are *E. coli* and *Klebsiella pneumonia* (K. *pneumonia*), these enzymes have also been identified in other members of the Enterobacteriaceae family.[6,8−10] In the 1980s and 1990s, *K. pneumoniae* was the bacterial species most likely to express ESBLs; however, in the 2000s *E. coli*-expressing ESBLs became dominant.[11−16] Various molecular methods may be used for detection and identification of genes encoding ESBL in various ESBL-producing

**Received:** November 28, 2018
**Accepted:** January 11, 2019

  

DOI: 10.1021/acs.analchem.8b05497
Anal. Chem. XXXX, XXX, XXX−XXX

species, including different assays based on PCR.[17−20] However, these genotypic tests are not in routine use, and they are usually performed for epidemiological studies.

Routinely, EBSL is detected phenotypically, which requires two steps. The first is the screening step, which is based on testing the organism for resistance to cephalosporin that is hydrolyzed by the three groups of ESBL. The second step is a conformity step, which is based on the fact that that all ESBLs are inhibited by clavulanate. In this step, a combination of the indicator cephalosporin and clavulanic acid must be established. These methods are time-consuming, requiring at least 48 h to obtain results.

ESBL test results are essential for appropriate and effective treatment. Random prescription of antibiotics by physicians before obtaining laboratory results may seriously affect the patient's outcome and contribute to further development of bacterial resistance to antibiotics. Thus, reducing the ESBL test time is highly crucial and may save patients' lives and potential spread. Ongoing studies are aimed at developing new, faster ways for detection of ESBL-producing bacteria such as MALDI-TOF.[21−23]

In this research, we used Fourier transform infrared spectroscopic (FTIR) microscopy in tandem with classifiers based on k-nearest neighbors (kNN) and polynomial support vector machines (SVM) as a potential tool for fast detection of ESBL-producing *E. coli* bacteria. Infrared spectroscopic techniques are noninvasive and can detect minor molecular and cellular changes associated with development of abnormality.[24] Such methods have been used for detection and identification of different biological entities such as bacteria, fungi, and different cancer tissues.[25] FTIR has also been applied effectively to study a variety of biological samples for the identification of different human diseases.[26−33] It has been successfully applied for detection, identification and taxonomic classification of bacteria such as *Escherichia coli*, Staphylococcus, and Bacillus.[34−42]

Recent studies highlighted the potential of IR spectroscopy, coupled with machine-learning algorithms, for following changes in bacterial cells under continuous exposure to kanamycin[43] and tetracycline[44] antibiotics. Our recently published studies demonstrated the potential of FTIR microscopy as a sensitive diagnostic tool for rapid identification of susceptibility of uropathogenic *E. coli* (UPEC) to antibiotics.[45,46]

## METHODOLOGY

**Bacterial Sample Collection.** For this study, 837 UPEC samples were obtained on MacConkey agar plates from the bacteriology laboratories in Soroka University Medical Center (SUMC). Each bacterial sample was obtained from a different patient and was represented by one FTIR spectrum only. The samples were identified at the species level by MALDI-TOF and were examined for ESBL-expression using disc tests. The samples were also examined by the routine assay (minimum inhibitory concentration, MIC) for susceptibility to the following antibiotics: ampicilin, cefuroxime, piperacillin, nitrofurantoin, ceftriaxone, gentamicin, ceftazidime, amoxicillin/clavul A, amikacin, cotrimoxazole, nalidixic acid, ofloxacin, piperacill/tazobact, ciprofloxacin, meropenem, and tobramycin.

**Sample Preparation for FTIR Microscopy Measurements.** Samples were picked up directly from bacterial colonies on the plates and placed on zinc-selenide slides, using a sterile bacteriological loop under sterile conditions. The samples were spread carefully on the slide, minimizing variations in thickness and enabling choice of the best site for spectral measurements.

**FTIR Measurements.** FTIR measurements were performed with an FTIR microscope (Nicolet -i10 infrared microscope) using a liquid-nitrogen-cooled mercury−cadmium-telluride (HgCdTe = MCT) detector, coupled to the FTIR spectrometer. To achieve a high signal-to-noise ratio (SNR), 128 coadded scans were collected in transmission mode for each sample, in the 600−4000 $cm^{-1}$ wavenumber region and at a spectral resolution of 4 $cm^{-1}$. A subset of the bacterial samples were examined three times on different days to assess reproducibly of the IR spectra. We measured at least 16 spectra from different sites of each bacterial sample. These acquisition parameters enabled us to obtain high quality and reproducible spectra.

**Spectral Preprocessing.** In well-established practice, various manipulations of the raw spectra are performed to enhance the SNR, improve discernment of the spectral features, and facilitate spectral interpretation and analysis and for comparison among spectra from samples with different thicknesses.[41] The acquired spectra were processed as follows: (1) Atmospheric compensation was applied to eliminate influences of $CO_2$ and air humidity. (2) The spectra were truncated to the range 900−1800 $cm^{-1}$, to exclude the water region at 3010−4000 $cm^{-1}$ as well as the region 1800−2800 $cm^{-1}$ where there are typically no spectroscopic features in biological samples. (3) The resulting spectra were then baseline-corrected, using the concave rubber-band method,[47] with 64 consecutive points and five iterations. Baseline correction eliminates variations due to shifts in baseline. By using the concave rubber-band correction method, we divided the spectrum into 64 equal-size ranges to construct the baseline. For absorbance spectra, the minimum *y*-value of the ranges is determined, and a polynomial function is fitted to these minimum points. Then we subtract this function from the spectrum to extract the baseline corrected spectrum. This procedure was repeated for the number of iterations. (4) The corrected spectra were then normalized using vector normalization followed by offset correction. Normalization of spectra eliminates the path length variation[48] and is a prerequisite for advanced statistical analysis of bacterial spectra.[49] We calculated the second derivative spectra using MATLAB with 13 smoothing points, and the resulting derivative spectra were used for further analysis.

**Statistical Analysis.** To differentiate between the $ESBL^+$ and $ESBL^-$ categories of *E. coli*, we tested several machine-learning algorithms: kNN,[50,51] SVM with polynomial kernel of the first-,[52] second-, and third-order. We performed numerous experiments to classify between the two categories using the mentioned classifiers with four different feature vectors: row data (i.e., absorption spectra); second derivative spectra; absorption spectra followed by PCA dimensionality reduction; second-derivative spectra followed by PCA. For assessment of potential accuracy, a 5-fold cross-validation approach was used. Using *K*-folds, the data is divided into *K* exclusive and even folds. The training set includes all of the folds except for one. Then the classification of the excluded fold is predicted and compared with the known classes. The procedure is repeated *K* times, once for each fold, and thus the statistical accuracy is estimated. This validation method is known to be optimistic when compared with testing a trained algorithm on a naive


DOI: 10.1021/acs.analchem.8b05497
Anal. Chem. XXXX, XXX, XXX−XXX

data set; nonetheless, the *K*-folds method is valuable for providing an initial indication of the potential of a new diagnostic, when the data set is not large enough to invoke separate training and testing sets for every set of conditions (i.e., for the multiple types of antibiotics). When the number of folds is equal to the data size, it is referred to a *leave one out* (LOO). The validation results are described using the confusion matrix in Table 1.

**Table 1. Confusion Matrix of the Binary Classifier**

| | | prediction | |
|---|---|---|---|
| | | positive state ($ESBL^+$) | negative state ($ESBL^-$) |
| true | positive state ($ESBL^+$) | TP | FN |
| | negative state ($ESBL^-$) | FP | TN |

Sensitivity (SE) is defined as TP/(TP + FN) , specificity (SP) is defined as TN/(FP + TN), and accuracy (Acc) is defined as (TP + TN)/(TP + FN + FP + TN). Positive-predictive value (PPV) is defined as TP/(TP + FP) while negative-predictive value (NPV) is defined as TN/(FN + TN).

## RESULTS AND DISCUSSION

In this study, we evaluated the potential of infrared spectroscopy in tandem with supervised machine-learning, SVM- and kNN-based classifiers, to classify 837 *E. coli* isolates as $ESBL^+$ or $ESBL^-$ in a few minutes following the first culture. For this goal, 569 $ESBL^-$ and 268 $ESBL^+$ *E. coli* isolates were examined by this spectroscopic method, under approval of the Institutional Review Helsinki Board at SUMC, in Beer-Sheva, Israel. All the examined UTI samples were identified as *E. coli* by MALDI-TOF and were classified into $ESBL^-$ or $ESBL^+$ by classical methods in the bacteriology lab at SUMC. There were no significant safety hazards or risks associated with this research.

Figure 1 shows the averaged spectra of $ESBL^-$ and $ESBL^+$ *E. coli* isolates in the 900−1800 $cm^{-1}$ region after preprocessing.

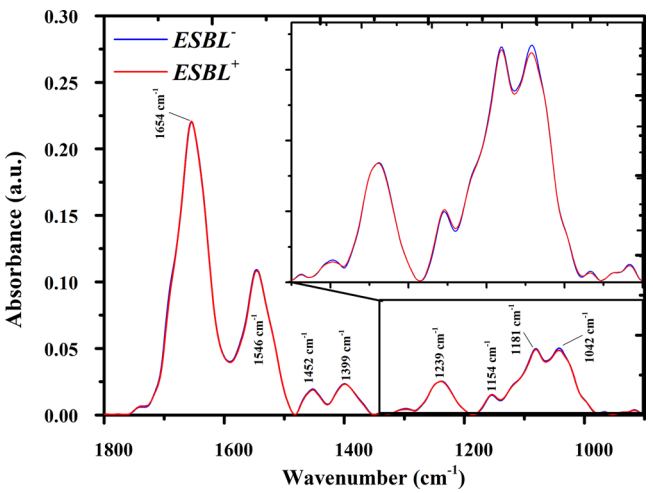


**Figure 1.** Average infrared absorption spectra of $ESBL^+$ and $ESBL^-$ *E. coli* isolates in the 900−1800 $cm^{-1}$ region after preprocessing. The main features of the absorption bands' spectra are labeled in the figure; subtle but repeatable differences are seen in the bands between 1000 and 1100 $cm^{-1}$.

The main features of the absorption bands are labeled in the figure. The Amide I (1691−1622 $cm^{-1}$),[53,54] Amide II (1558−1520 $cm^{-1}$),[55] and Amide III (1310−1240 $cm^{-1}$)[55,56] bands are associated mainly with the stretching vibrations of protein functional groups: N−H, C−N, and C═O. The region 1471−1430 $cm^{-1}$ is associated mainly with bending vibrations of lipid functional groups C−H and $CH_2$.[53,55] The 1200−1272 $cm^{-1}$ region is mainly associated with nucleic acid functional groups $PO_2$ and P═O and their stretch modes.[55,56] The 900−1200 $cm^{-1}$ region is associated mainly with carbohydrates functional groups C−O−C, C−O, C−O−P, and P−O−P and the associated stretch vibrations.[53,55,56]

The subtle spectral differences that can be seen from Figure 1, between $ESBL^-$ and $ESBL^+$ isolates, are not surprising, because, in many cases, bacteria can develop resistance to a specific antibiotic due to point mutations in their genome.[57,58] Nonetheless, these changes were repeatedly detected by infrared spectroscopy, for which the ability to monitor minute molecular changes associated with developing resistivity has been proved.[24,46,59−64] Figure S-1 shows an inset of the spectral region 950−1200 $cm^{-1}$ of Figure 1, where the observable differences manifest.

Due to the small spectral differences between $ESBL^-$ and $ESBL^+$, appropriate sample preparation is needed to yield a strong infrared signal. Moreover, it is important to acquire high-SNR spectra that are highly reproducible. Each of the spectra included in this study is an average of at least 16 spectra measured from different sites of the same sample (data not shown) in order to optimize the accuracy.

To check the variation among different sample preparations of the same sample, spectra acquired from different colonies of *E. coli* originating from the same plate are plotted in Figure 2a. As can be seen from this figure, the variance among the three spectra was small. The three samples were prepared and measured on the same day using the same parameters. In addition, when the same colony was measured on different days, the spectra were almost identical, as can be seen in Figure 2b.

Moreover, although the spectra of $ESBL^-$ and $ESBL^+$ *E. coli* are highly similar and predominantly overlap (Figure 1), the subtle spectral changes in the relative intensities and shapes in the functional groups of the infrared spectrum invoke no band shifts. Therefore, we chose variations of two different supervised machine-learning classifier algorithms to analyze the ESBL-producing UPEC isolates as described in Methodology.

Figure 3 displays the receiver operating characteristic (ROC) curve based on the kNN classifier for ESBL-producing bacteria, using second-derivative spectra followed by PCA, which gave the best classification results. The ROC curve is a convenient way to illustrate the performance of a binary classifier, where the area under the curve (AUC) represents the accuracy of the classifier. In our analysis, we defined $ESBL^+$ as the "positive" state and the $ESBL^-$ as the "negative" state. The different classifier performances are summarized in Table 2.

As can be seen from Figure 1 and Table 2, even though the spectral differences between $ESBL^+$ and $ESBL^-$ spectra are subtle, they are sufficiently repeatable to achieve good classification performance to distinguish the two categories of the spectra. This is an indication that FTIR microscopy is highly sensitive for monitoring minor cellular biomolecular changes[47,48] associated with developing resistivity to specific antimicrobial agents.



DOI: 10.1021/acs.analchem.8b05497
*Anal. Chem.* XXXX, XXX, XXX−XXX

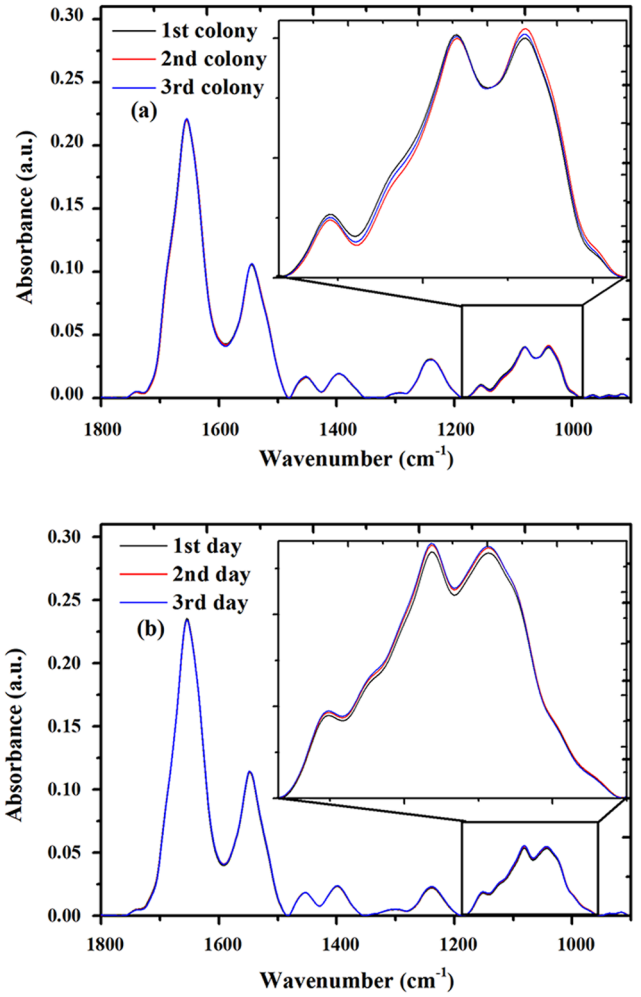


**Figure 2.** (a) IR average spectra acquired from different colonies of the same isolate. Each line belongs to different single colony. All the samples were prepared and measured on the same day using the same parameters. (b) IR average spectra acquired from the same colony at different days. All the spectra are plotted in the 900−1800 $cm^{-1}$ region after preprocessing.

Although the predominant mechanism of resistance to $\beta$-lactams antibiotics in Gram-negative bacteria, including *E. coli*, is the production of $\beta$-lactamases, there are other resistance mechanisms of $\beta$-lactam antibiotics that are not related to $\beta$-lactamase activity.[65] Therefore, in the following analysis, we evaluated the potential of this spectroscopic method to differentiate between *E. coli* isolates that are resistant to ampicillin in the context of their mechanism of acquiring the resistivity: an ESBL-producing mechanism or other mechanisms. The obtained data from the bacteriology lab at SUMC for tested samples included the susceptibility to more than 10 different antibiotics (regardless of the mechanism), in addition to an ESBL test as positive or negative.

For this goal, the averages of the 268 samples of $ESBL^+$ were compared to 335 samples that were $ESBL^-$ and still resistant to ampicillin. These are displayed in Figure 4. As can be seen, the spectral differences between the two classes are again small, with subtle changes in the relative intensities and shapes in the functional groups but with no band shifts. The major differences are in the carbohydrate region 1000−1100 $cm^{-1}$. Figure S-2 shows an inset of the spectral region 950−1200 $cm^{-1}$ from Figure 4, where the observable differences are manifest.

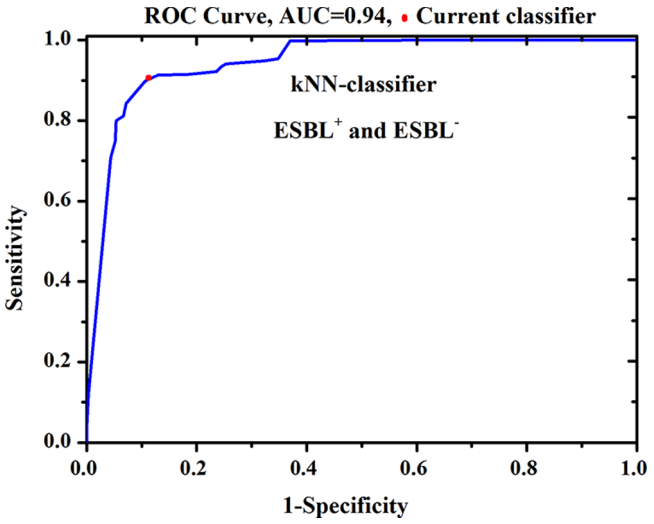


**Figure 3.** Resulting ROC for classifying the *E. coli* isolates into $ESBL^+$ and $ESBL^-$ categories using second derivative spectra followed by PCA.

**Table 2. Different Classifier Performances for Classifying the *E. coli* Isolates Based on Production of $\beta$-Lactamases as $ESBL^+$ and $ESBL^-$ [a]**

| | feature vector | SE | SP | Acc | PPV | NPV |
|---|---|---|---|---|---|---|
| SVM linear | raw data | 0.93 | 0.39 | 0.76 | 0.76 | 0.72 |
| SVM−quadratic | PCA, second derivative | 0.97 | 0.60 | 0.85 | 0.84 | 0.91 |
| SVM−cubic | second derivative | 0.92 | 0.79 | 0.87 | 0.90 | 0.81 |
| SVM−cubic | PCA, second derivative | 0.98 | 0.65 | 0.88 | 0.86 | 0.95 |
| KNN | PCA, second derivative | 0.99 | 0.94 | 0.98 | 0.97 | 0.99 |

[a]SE, Sensitivity; SP, specificity; Acc, accuracy; PPV, positive-predictive value; NPV, negative-predictive value.

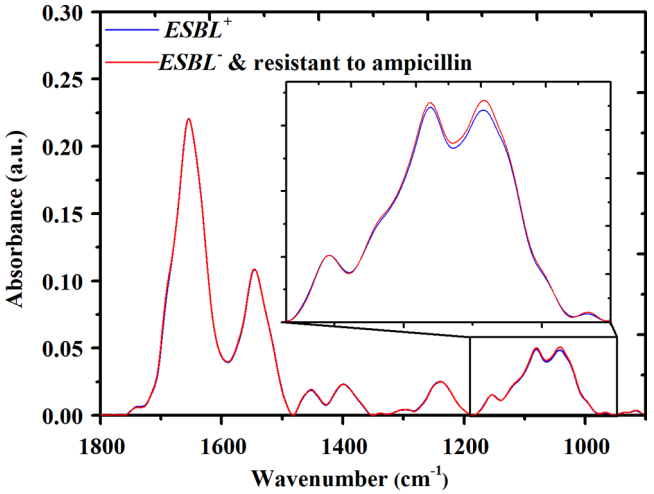


**Figure 4.** Average infrared absorption spectra of *E. coli* isolates that are resistant to ampicillin in the 900−1800 $cm^{-1}$ region after preprocessing.



DOI: 10.1021/acs.analchem.8b05497
Anal. Chem. XXXX, XXX, XXX−XXX

In our previous studies,[46,60] the differences due to susceptibility are referred to as intervariance (differences between the resistance and sensitive classes), while the differences due to different mechanisms of acquiring resistivity are referred to as intravariance (differences among the samples belonging to the same class).

In the following analysis the differentiation is between the *E. coli* isolates that are resistant to ampicillin as producing and nonproducing ESBL (i.e., different mechanisms of acquiring resistance to ampicillin). Thus, the differences due to the mechanisms of resistance become intervariance. Figure 5

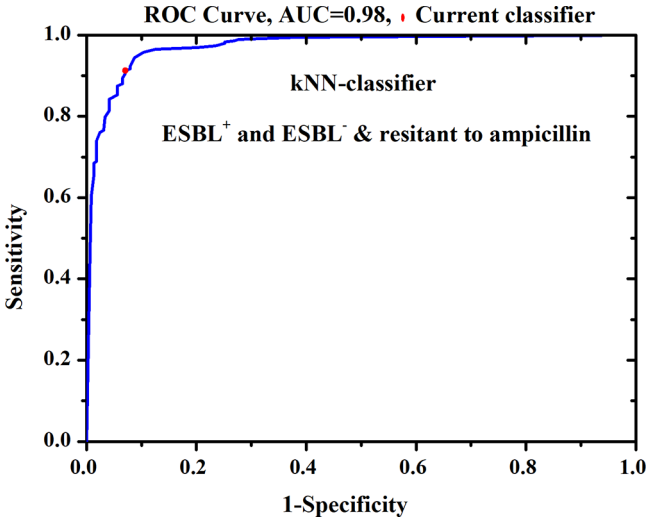


**Figure 5.** Resulting ROC for classifying the *E. coli* isolates into ESBL$^+$ and ESBL$^-$ and resistant to ampicillin using second derivative spectra followed by PCA.

displays the ROC curve for the kNN classifier for the classes of ESBL-producing and nonproducing variants. We defined ESBL$^+$ as the "positive" state and the ESBL$^-$ yet-resistant-to-ampicillin as the "negative" state. The different machine-learning classifiers' performances are summarized in Table 3.

**Table 3. SVM Classifier Performances for Classifying *E. coli* Isolates as ESBL$^+$ and ESBL$^-$ but Resistant to Ampicillin[a]**

| | feature vector | SE | SP | Acc | PPV | NPV |
|---|---|---|---|---|---|---|
| SVM linear | raw data | 0.78 | 0.59 | 0.70 | 0.70 | 0.66 |
| SVM−quadratic | PCA of the raw data | 0.79 | 0.66 | 0.73 | 0.75 | 0.70 |
| SVM−cubic | second derivative | 0.78 | 0.83 | 0.85 | 0.86 | 0.84 |
| SVM−cubic | PCA, second derivative | 0.94 | 0.91 | 0.93 | 0.92 | 0.93 |
| KNN | PCA, second derivative | 0.94 | 0.93 | 0.94 | 0.94 | 0.93 |

[a]SE, sensitivity; SP, specificity; Acc, accuracy; PPV, positive-predictive value; NPV, negative-predictive value.

Again here, and as can be seen from Figure 5 and Table 3, even though the spectral differences between ESBL$^+$ and ESBL$^-$ and resistant to ampicillin are subtle, they are still sufficiently repeatable to achieve a good classification values between these two categories.

As mentioned in the introduction, recent studies aimed at developing fast assays for detection of ESBL-producing bacteria include the use of MALDI-TOF.[21,22,66] These studies reported promising findings. However, due to the fact that MALDI-TOF is based on protein mass differences,[67] it is complicated to deal with all of the types and subtypes of existing ESBLs. Moreover, any changes in the protein mass of these ESBL isoforms due to frequent random mutations (which might not affect the activity of these enzymes) can lead to incorrect identification by MALDI-TOF. On the other hand, the FTIR spectroscopic technique is independent of the protein mass difference, and enlarging the database to include all the various types and subtypes of existing ESBLs, as well as new mutations may assist in management of this problem. Furthermore, infrared microscopy has additional advantages over MALDI: it is simpler, is less expensive, and can be used for all types of bacteria.

In summary, the promising results obtained in this study are complementary to our previous studies,[46,60] which demonstrated the potential of the FTIR microscopy method to successfully identify the susceptibility of *E. coli* to different antibiotics regardless of the mechanism of antibiotic resistance.

## CONCLUSIONS

Infrared spectroscopy, coupled with machine-learning classification algorithms for pattern recognition, can serve as a powerful tool to determine whether *E. coli* isolates are ESBL-producing, in a time span of minutes following the first culture. The results of this study indicate promise for this spectroscopic method to differentiate between different mechanisms of acquired resistance to antibiotics.

## ASSOCIATED CONTENT

### Supporting Information

The Supporting Information is available free of charge on the ACS Publications website at DOI: 10.1021/acs.analchem.8b05497

The spectral differences used by our classifiers to differentiate between ESBL$^+$ and ESBL$^-$ *E. coli* isolates weresubtle; thus, it is helpful to magnify spectral regions where there are observable differences. Figure S-1 plots the averages of ESBL$^+$ vs ESBL$^-$ *E. coli* isolates in the spectral region 950 1200 cm$^{-1}$. Figure S-2 plots the averages of *E.coli* spectra categorized as of ESBL$^+$ or ESBL$^-$ yet resistant to ampicillin, in the spectral region 950 1200 cm$^{-1}$ (PDF)

## AUTHOR INFORMATION

### Corresponding Authors

*Tel: +972-8-6475794; fax: +972-8-851916; e-mail: ahmad@sce.ac.il.

*Tel: +972-8-6479867; fax: +972-8-6479867; e-mail: mahmoudh@bgu.ac.il.

### ORCID

Ahmad Salman: 0000-0003-4953-8648

### Author Contributions

▲These authors contributed equally.

### Notes

The authors declare no competing financial interest.

## ACKNOWLEDGMENTS

Financial support by SCE internal research funding is gratefully acknowledged.



DOI: 10.1021/acs.analchem.8b05497
Anal. Chem. XXXX, XXX, XXX−XXX

## REFERENCES


(1) Percival, S. L.; Williams, D.; Cooper, T.; Randle, J. *Biofilms in infection prevention and control: A healthcare handbook*; Academic Press: Boston, 2014.
(2) Hertz, F. B. *ESBL-producing Escherichia Coli: Antibiotic Selection, Risk Factors and Population Structure*; University of Copenhagen, Faculty of Science, Department of Biology, Functional Genomics: Copenhagen, 2014.
(3) Peirano, G.; Pitout, J. D. *Int. J. Antimicrob. Agents* **2010**, *35*, 316−321.
(4) Bush, K.; Jacoby, G. A. *Antimicrob. Agents Chemother.* **2010**, *54*, 969−976.
(5) Rogers, B. A.; Sidjabat, H. E.; Paterson, D. L. *J. Antimicrob. Chemother.* **2011**, *66*, 1−14.
(6) Pitout, J. D.; Laupland, K. B. *Lancet Infect. Dis.* **2008**, *8*, 159−166.
(7) Tansarli, G. S.; Poulikakos, P.; Kapaskelis, A.; Falagas, M. E. *J. Antimicrob. Chemother.* **2014**, *69*, 1177−1184.
(8) Naseer, U.; Sundsfjord, A. *Microb. Drug Resist.* **2011**, *17*, 83−97.
(9) Paterson, D. L.; Bonomo, R. A. *Clin. Microbiol. Rev.* **2005**, *18*, 657−686.
(10) Chong, Y.; Shimoda, S.; Shimono, N. *Infect., Genet. Evol.* **2018**, *61*, 185−188.
(11) Rice, L. B. *Curr. Opin. Microbiol.* **2009**, *12*, 476−481.
(12) Falagas, M.; Karageorgopoulos, D. E. *Journal of Hospital Infection* **2009**, *73*, 345−354.
(13) Bush, K. *Curr. Opin. Microbiol.* **2010**, *13*, 558−564.
(14) Cantón, R.; González-Alba, J. M.; Galán, J. C. *Front. Microbiol.* **2012**, *3*, 110.
(15) Pitout, J. D. *Expert Rev. Anti-Infect. Ther.* **2012**, *10*, 1165−1176.
(16) Pitout, J. D. *Front. Microbiol.* **2012**, *3*, 9.
(17) M'Zali, F.-H.; Gascoyne-Binzi, D. M.; Heritage, J.; Hawkey, P. M. *J. Antimicrob. Chemother.* **1996**, *37*, 797−802.
(18) Kim, J.; Lee, H.-J. *Antimicrob. Agents Chemother.* **2000**, *44*, 1860−1864.
(19) Randegger, C. C.; Hächler, H. *Antimicrob. Agents Chemother.* **2001**, *45*, 1730−1736.
(20) Chanawong, A.; M'Zali, F. H.; Heritage, J.; Lulitanond, A.; Hawkey, P. M. *Antimicrob. Agents Chemother.* **2001**, *45*, 2110−2114.
(21) Ferrer, R.; Martin-Loeches, I.; Phillips, G.; Osborn, T. M.; Townsend, S.; Dellinger, R. P.; Artigas, A.; Schorr, C.; Levy, M. M. *Crit. Care Med.* **2014**, *42*, 1749−1755.
(22) Cizmeci, Z.; Otlu, B.; Aktaş, E.; Ördekçi, S.; Açıkgöz, Ö.; Güleç, N. *Mikrobiyol. Bul.* **2018**, *52*, 13−22.
(23) Espinosa, R. F.; Rumi, V.; Marchisio, M.; Cejas, D.; Radice, M.; Vay, C.; Barrios, R.; Gutkind, G.; Di Conza, J. *J. Microbiol. Methods* **2018**, *148*, 22−28.
(24) Jin, N.; Zhang, D.; Martin, F. L. *Integr. Biol.* **2017**, *9*, 406−417.
(25) Baker, M. J.; Trevisan, J.; Bassan, P.; Bhargava, R.; Butler, H. J.; Dorling, K. M.; Fielden, P. R.; Fogarty, S. W.; Fullwood, N. J.; Heys, K. A.; et al. *Nat. Protoc.* **2014**, *9*, 1771.
(26) Matthäus, C.; Bird, B.; Miljković, M.; Chernenko, T.; Romeo, M.; Diem, M. *Methods Cell Biol.* **2008**, *89*, 275−308.
(27) Mostaço-Guidolin, L. B.; Bachmann, L. *Appl. Spectrosc. Rev.* **2011**, *46*, 388−404.
(28) Kelly, J. G.; Nakamura, T.; Kinoshita, S.; Fullwood, N. J.; Martin, F. L. *Analyst* **2010**, *135*, 3120−3125.
(29) Mordechai, S.; Shufan, E.; Katz, B. P.; Salman, A. *Analyst* **2017**, *142*, 1276−1284.
(30) Ildiz, G. O.; Arslan, M.; Unsalan, O.; Araujo-Andrade, C.; Kurt, E.; Karatepe, H.; Yilmaz, A.; Yalcinkaya, O.; Herken, H. *Spectrochim. Acta, Part A* **2016**, *152*, 551−556.
(31) Staniszewska-Slezak, E.; Fedorowicz, A.; Kramkowski, K.; Leszczynska, A.; Chlopicki, S.; Baranska, M.; Malek, K. *Analyst* **2015**, *140*, 2273−2279.
(32) Yu, M.-C.; Rich, P.; Foreman, L.; Smith, J.; Yu, M.-S.; Tanna, A.; Dibbur, V.; Unwin, R.; Tam, F. W. *Sci. Rep.* **2017**, *7*, 4601.
(33) Titus, J.; Viennois, E.; Merlin, D.; Unil Perera, A. *J. Biophotonics* **2017**, *10*, 465−472.
(34) Burgula, Y.; Khali, D.; Kim, S.; Krishnan, S.; Cousin, M.; Gore, J.; Reuhs, B.; Mauer, L. *J. Food Prot.* **2006**, *69*, 1777−1784.
(35) Kim, S.; Burgula, Y.; Ojanen-Reuhs, T.; Cousin, M. A.; Reuhs, B. L.; Mauer, L. J. *J. Food Sci.* **2006**, *71*, 57−61.
(36) Lamprell, H.; Mazerolles, G.; Kodjo, A.; Chamba, J.; Noel, Y.; Beuvier, E. *Int. J. Food Microbiol.* **2006**, *108*, 125−129.
(37) Filip, Z.; Herrmann, S.; Kubat, J. *Microbiol. Res.* **2004**, *159*, 257−262.
(38) Burgula, Y.; Khali, D.; Kim, S.; Krishnan, S.; Cousin, M.; Gore, J.; Reuhs, B.; Mauer, L. *J. Food Prot.* **2006**, *69*, 1777−1784.
(39) Rebuffo, C. A.; Schmitt, J.; Wenning, M.; von Stetten, F.; Scherer, S. *Appl. Environ. Microbiol.* **2006**, *72*, 994−1000.
(40) Rebuffo-Scheer, C. A.; Schmitt, J.; Scherer, S. *Appl. Environ. Microbiol.* **2007**, *73*, 1036−1040.
(41) Salman, A.; Pomerantz, A.; Tsror, L.; Lapidot, I.; Moreh, R.; Mordechai, S.; Huleihel, M. *Analyst* **2012**, *137*, 3558−3564.
(42) Kim, J.; Schmid-Burgk, W.; Claus, D.; Kornhuber, H. *Arch. Psychiatr. Nervenkrankh.* **1982**, *232*, 299−304.
(43) Jin, N.; Paraskevaidi, M.; Semple, K. T.; Martin, F. L.; Zhang, D. *Anal. Chem.* **2017**, *89*, 9814−9821.
(44) Jin, N.; Semple, K. T.; Jiang, L.; Luo, C.; Zhang, D.; Martin, F. L. *Analyst* **2018**, *143*, 768−776.
(45) Sharaha, U.; Rodriguez-Diaz, E.; Riesenberg, K.; Bigio, I. J.; Huleihel, M.; Salman, A. *Anal. Chem.* **2017**, *89*, 8782−8790.
(46) Salman, A.; Sharaha, U.; Rodriguez-Diaz, E.; Shufan, E.; Riesenberg, K.; Bigio, I. J.; Huleihel, M. *Analyst* **2017**, *142*, 2136−2144.
(47) Salman, A.; Shufan, E.; Zeiri, L.; Huleihel, M. *Biochim. Biophys. Acta, Gen. Subj.* **2013**, *1830*, 2720−2727.
(48) Pomerantz, A.; Cohen, Y.; Shufan, E.; Ben-Naim, Y.; Mordechai, S.; Salman, A.; Huleihel, M. *J. Photochem. Photobiol., B* **2014**, *141*, 308−314.
(49) Salman, A.; Shufan, E.; Lapidot, I.; Pomerantz, A.; Huleihel, M.; Tsror, L.; Moreh, R.; Mordechai, S. *J. Biomed. Opt.* **2012**, *17*, 017002.
(50) Manocha, S.; Girolami, M. A. *Pattern Recognition Letters* **2007**, *28*, 1818−1824.
(51) Bishop, C. M. *Neural networks for pattern recognition*; Oxford University Press, Inc., 1996; p 482.
(52) Cortes, C.; Vapnik, V. *Machine learning* **1995**, *20*, 273−297.
(53) Davis, R.; Mauer, L. *Current research, technology and education topics in applied microbiology and microbial biotechnology* **2010**, *2*, 1582−1594.
(54) Vapnik, V. *Statistical learning theory*; Wiley: New York, 1998; Vol. 3.
(55) Beekes, M.; Lasch, P.; Naumann, D. *Vet. Microbiol.* **2007**, *123*, 305−319.
(56) Fujioka, N.; Morimoto, Y.; Arai, T.; Kikuchi, M. *Cancer Detect. Prev.* **2004**, *28*, 32−36.
(57) Alekshun, M. N.; Levy, S. B. *Cell* **2007**, *128*, 1037−1050.
(58) Walsh, C. *Nature* **2000**, *406*, 775−781.
(59) Martin, F. L.; Kelly, J. G.; Llabjani, V.; Martin-Hirsch, P. L.; Patel, I. I.; Trevisan, J.; Fullwood, N. J.; Walsh, M. J. *Nat. Protoc.* **2010**, *5*, 1748.
(60) Sharaha, U.; Rodriguez-Diaz, E.; Riesenberg, K.; Bigio, I. J.; Huleihel, M.; Salman, A. *Anal. Chem.* **2017**, *89*, 8782−8790.
(61) Beekes, M.; Lasch, P.; Naumann, D. *Vet. Microbiol.* **2007**, *123*, 305−319.
(62) Levin, I. W.; Bhargava, R. *Annu. Rev. Phys. Chem.* **2005**, *56*, 429−474.
(63) Lechowicz, L.; Urbaniak, M.; Adamus-Bialek, W.; Kaca, W. *Acta Biochim. Pol.* **2013**, *60*, 713−718.
(64) Neu, H. C. *Science* **1992**, *257*, 1064−1073.
(65) Schmieder, R.; Edwards, R. *Future Microbiol.* **2012**, *7*, 73−89.
(66) Espinosa, R. F.; Rumi, V.; Marchisio, M.; Cejas, D.; Radice, M.; Vay, C.; Barrios, R.; Gutkind, G.; Di Conza, J. *J. Microbiol. Methods* **2018**, *148*, 22−28.
(67) Wieser, A.; Schneider, L.; Jung, J.; Schubert, S. *Appl. Microbiol. Biotechnol.* **2012**, *93*, 965−974.



DOI: 10.1021/acs.analchem.8b05497
*Anal. Chem.* XXXX, XXX, XXX−XXX